Interfacial degradation effects of aqueous solution-processed molybdenum trioxides on the stability of organic solar cells evaluated by a differential method

5 AUTHORS, INCLUDING:

Zhao-Kui Wang
Soochow University (PRC)
89 PUBLICATIONS   452 CITATIONS

SEE PROFILE

Hiroyuki Okada
University of Toyama
153 PUBLICATIONS   1,300 CITATIONS

SEE PROFILE

L. S. Liao
Soochow University, Suzhou, China
181 PUBLICATIONS   3,247 CITATIONS

SEE PROFILE

Interfacial degradation effects of aqueous solution-processed molybdenum trioxides on the stability of organic solar cells evaluated by a differential method

Yan-Hui Lou, Zhao-Kui Wang, Da-Xing Yuan, Hiroyuki Okada, and Liang-Sheng Liao

---

Articles you may be interested in

Efficiency enhancement in solution-processed organic small molecule: Fullerene solar cells via solvent vapor annealing
Appl. Phys. Lett. **106**, 183302 (2015); 10.1063/1.4919707

Evaporation-free inverted organic photovoltaics using a mixture of silver nanoparticle ink formulations for solution-processed top electrodes
Appl. Phys. Lett. **105**, 233901 (2014); 10.1063/1.4903893

On the kinetics of MoSe2 interfacial layer formation in chalcogen-based thin film solar cells with a molybdenum back contact
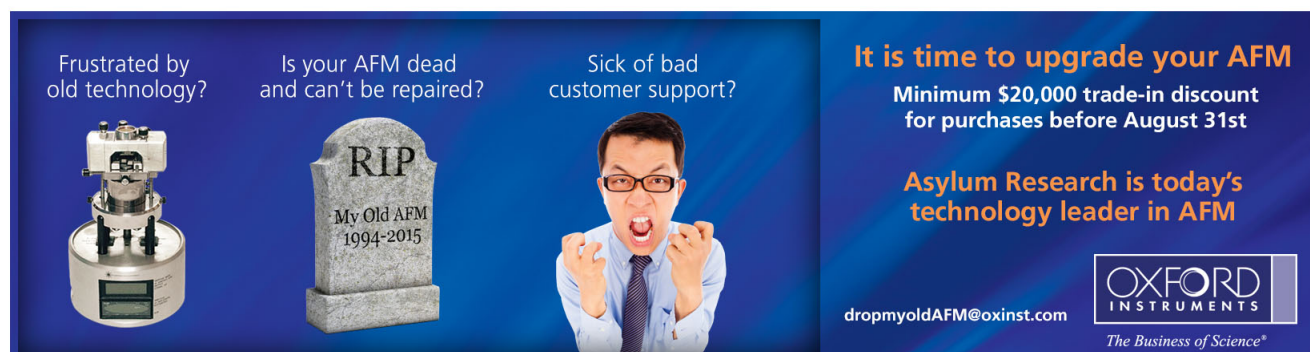Appl. Phys. Lett. **102**, 091907 (2013); 10.1063/1.4794422

Small molecule solution-processed bulk heterojunction solar cells with inverted structure using porphyrin donor
Appl. Phys. Lett. **102**, 013305 (2013); 10.1063/1.4773910

Exciton dissociation and charge trapping at poly(3-hexylthiophene)/phenyl-C61-butyric acid methyl ester bulk heterojunction interfaces: Photo-induced threshold voltage shifts in organic field-effect transistors and solar cells
J. Appl. Phys. **111**, 084908 (2012); 10.1063/1.4705277

Interfacial degradation effects of aqueous solution-processed molybdenum trioxides on the stability of organic solar cells evaluated by a differential method

Yan-Hui Lou,[1,2] Zhao-Kui Wang,[1,a)] Da-Xing Yuan,[1] Hiroyuki Okada,[2] and Liang-Sheng Liao[1,a)]

[1]*Institute of Functional Nano & Soft Materials (FUNSOM), Soochow University, Suzhou, Jiangsu 215123, China*
[2]*Graduate School of Science and Technology, University of Toyama, 3190 Gofuku Toyama, Japan*

The authors investigate the influence of two hole interfacial materials poly (3,4-ethylenedioxythiophene):poly (styrenesulfonate) (PEDOT:PSS) and aqueous solution-processed MoO_3 ($sMoO_3$) on cell stability. $sMoO_3$-based device demonstrated obviously improved stability compared to PEDOT:PSS-based one. Current-voltage characteristics analysis is carried out to investigate the effect of the hole interfacial layers on the cell stability. The formation of additional trap states at the interfaces between the hole interfacial layer and the active layer in degraded devices is verified by a differential method. Improved cell stability is attributed to a relatively stable $sMoO_3$ interfacial layer compared to PEDOT:PSS by comparing their different trap states distributions. © *2014 AIP Publishing LLC*. [http://dx.doi.org/10.1063/1.4895805]

Large improvements in power conversion efficiency (PCE) and the cell reliability of Polymer-fullerene based organic solar cells (OSCs) are desired for commercialization application.[1–3] Particularly, the issue of cell stability has to be paid more attentions when the power conversion efficiency is approaching 10%. Great efforts have been taken in the cell stability especially the materials stability, such as the active layer,[4,5] the electrodes,[6,7] the electron transport layer,[8,9] and the hole transport layer.[10,11] The physical stabilities such as the interfacial condition,[12,13] the cell structure,[14] and even the film processing means also play important roles in the whole cell degradation.[15] Generally, cell reliability is dependent on a combined effect of aforementioned channels. However, the hole transport layer and its related interface conditions are regarded to be the most important factors that affect the whole cell reliability.[10–13,16,17]

Poly (3,4-ethylenedioxythiophene):poly (styrenesulfonate) (PEDOT:PSS) is one of mostly used hole transport materials in OSCs by its good conductivity and solution processability. Nevertheless, the device stability is seriously restricted by the hygroscopic nature of the aqueous PEDOT:PSS dispersions.[18,19] Recently, solution-processed transition metal oxides (TMOs), such as Molybdenum oxide (MoO_3), Vanadium oxide (V_2O_5), Germanium dioxide (GeO_2), and nickel oxide (NiO), have been widely used in OSCs for avoiding the acidic nature of the aqueous PEDOT:PSS dispersions.[20–29] As predicted, most TMO-based OSCs exhibited prolonged lifetime compared to those PEDOT:PSS based devices. However, the detailed degradation mechanisms related to the hole interfacial layer are not yet well understood. Many methods have been developed to investigate the intrinsic factors of device degradation.[30–32] Differential method, enabling one to extract quantitative information about an arbitrary energetic distribution of traps for current carriers,[33] is a simple technique that can

evaluate the space charge, the trap state, and the density of states (DOS) in amorphous and organic semiconductor films just based on a measurement of current-voltage (*I-V*) characteristics.[33–37] Several limits and/or assumptions, such as that the concentration of free carriers should be much smaller than that of trapped ones, and that the application to non-steady-state currents may give rise to substantial inaccuracies, should be considered when using this technique.[33] Nevertheless, the energy dependent DOS calculated by this technique can provide some interfacial information quantitatively since the calculation is originated from a basic *I-V* characteristics.

In this letter, we investigate the effect of hole transport layers (PEDOT:PSS and aqueous solution-processed MoO_3 ($sMoO_3$)) on the stability of polymer: fullerene bulk heterojunction solar cells. Differential method is used to evaluate the energy dependent DOS distribution during the cell degradation process. $sMoO_3$-based OSCs demonstrate obvious improvement of cell reliability compared with PEDOT:PSS-based ones. Direct evidence of interface degradation resulted from the PEDOT:PSS interfacial layer is obtained from the shape change of energy dependent DOS distribution.

MoO_3 powder ($\sim$50 nm in particle size) was purchased from Nichem Fine Technology Co. Ltd. (Taiwan). It was directly dissolved into the deionized water for getting the MoO_3 aqueous solution (with an optimized concentration of 0.08 wt. %). Over 24 h stirring under 70 °C are necessary for preparing the MoO_3 aqueous solution. MoO_3 and PEDOT:PSS solution were spin-coated onto the ITO substrates at 4000 rpm for 60 s and annealed at 120 °C for 10 min in air. The resulting $sMoO_3$ film has a thickness about 5 nm and a surface roughness (in Root Mean Square, RMS) of 3.2 nm. The active layer was spin-coated at 700 rpm for 50 s from a solution of poly (3-hexylthiophene) (P3HT):indene-C_{60} bisadduct ($IC_{60}BA$) (19 mg/ml, 1:1 by volume) in dichlorobenzene in the glove box. The LiF (0.5 nm) and Al (100 nm) were deposited, respectively, in a vacuum deposition chamber under a pressure about

a)Electronic addresses: zkwang@suda.edu.cn and lsliao@suda.edu.cn

2×10^{-6} Torr. *I-V* characteristics under 1 sun illumination were performed in N_2 glove box using a programmable Keithley 2400 source meter under AM 1.5G solar irradiation at 100 mW cm^{-2}. The cell stabilities were evaluated under continuous irradiation by an incandescent lamp (in intensity of 52 mW cm^{-2}) in air under ambient conditions without encapsulation.

The *J-V* characteristics of *s*MoO$_3$- and PEDOT:PSS-based OSCs under AM 1.5G illumination with light intensity of 100 mW cm^{-2} were shown in Fig. 1. The reference device using PEDOT:PSS as an ITO modification layer showed a PCE of 5.43% with an open circuit voltage (V_{oc}) of 0.77 V, a short circuit current density (J_{sc}) of 13.46 mA cm^{-2}, and a fill factor (FF) of 52%, respectively. The *s*MoO$_3$-based device exhibited a slightly improved PCE of 5.54% with V_{oc} of 0.75 V, J_{sc} of 13.82 mA cm^{-2}, and FF of 53%, respectively. It suggests that aqueous solution-processed *s*MoO$_3$ film can act as an efficient anode interfacial layer in OSCs by replacing of PEDOT:PSS.

Interfacial layer plays very important role in the stability of OSCs. Several key issues, such as device fabricating circumstance, chemical interaction between the interfacial layer and the metal electrode, and the atom diffusion, are regarded as the main factors that affect the device degradation.[38] Especially for a wet process (e.g., spin-coating presently), solvents may remain in the organic film even if a baking is carried out.[16] That's why the strong acidic nature of PEDOT:PSS would corrode ITO electrode and deteriorate the cell stability. Zilberberg *et al.* also reported that a solution-processable MoO$_x$ based OSCs show dramatically improved stability and after 30 days retain 90% of their initial PCE in N_2 and 84% in air.[26] Different from their work ((based on sol-gel processing), we reported a more simple and environment-friendly processing (aqueous solution-processable route) for depositing MoO$_3$ film. In present work, the pH value of MoO$_3$ aqueous solution was about 4, which is higher than that of aqueous PEDOT:PSS dispersions ($\sim$1). Therefore, improved device stability is expected to be achieved in *s*MoO$_3$-based devices compared to the PEDOT:PSS-based ones. Fig. 2 shows the normalized cell parameters including PCE, V_{oc}, J_{sc}, and FF as
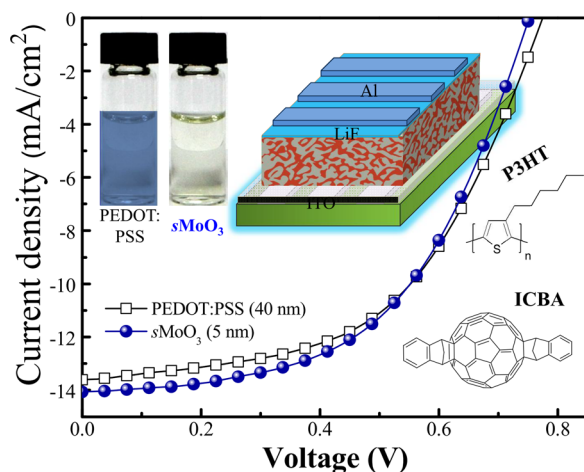
a function of time in PEDOT:PSS- and *s*MoO$_3$-based OSCs. PEDOT:PSS-based cell decayed rapidly in initial 150 min, resulting in almost 90% decrease in PCE; whereas, just 40% decrease in PCE was observed in *s*MoO$_3$-based one. After 300 min continuous light-soaking, *s*MoO$_3$-based cell still kept half value of initial PCE. In contrast, nearly no PCE appeared in PEDOT:PSS-based device. The degradation condition of V_{oc}, J_{sc}, and FF shown in Fig. 2(b) indicated that partly restrained PCE deterioration in *s*MoO$_3$-based cell is attributed to relatively slow decays of J_{sc} and V_{oc}. It is easily understood that the drop of J_{sc} mainly stems from the loss in absorption due to the active layer degradation with time.[39,40] Although the factors that affect the V_{oc} have yet to be clearly established, there is a common view that V_{oc} is determined by the difference of the work functions of two electrodes when the electrodes contact the active layer non-ohmically. We assume that the improved V_{oc} in *s*MoO$_3$-based cell was related to a more stable *s*MoO$_3$ interface compared to PEDOT:PSS-based one.

To verify the aforementioned assumption, the evaluation of *J-V* characteristics in *s*MoO$_3$- and PEDOT:PSS-based OSCs (Fresh and 1 h degraded devices) in dark conditions was carried out. Figs. 3(a) and 3(b) shows the corresponding *J-V* curves for log *J*-*V* plots and log *J*-log *V* plots, respectively. In the fresh devices, the *J-V* characteristics demonstrated very stable currents and excellent rectification behaviors. Particularly, log *J*-log *V* plots show a very normal forward characteristics for both *s*MoO$_3$- and PEDOT:PSS-based fresh devices. In the low bias region ($<$0.3 V), the slope of log *J*-log *V* curves is about 1, corresponding to an ohmic-like injection behavior. The currents rise suddenly with voltage with a slope about 5 in the mid-voltage region (0.3–0.7 V) and

FIG. 1. Typical *J-V* characteristics in *s*MoO$_3$ (5 nm) and PEDOT:PSS (40 nm) based solar cells under a simulated AM 1.5G spectrum illumination (100 mW cm^{-2}). Inset is the photos of MoO$_3$ aqueous solutions, a schematic device structure, and the molecular structures under investigation.
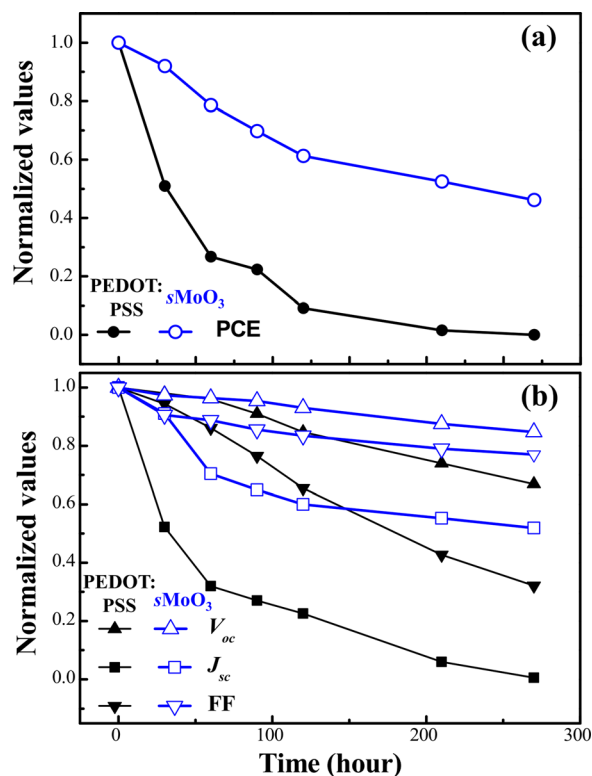

FIG. 2. The normalized PCE values (a) and other cell parameters (b) as a function of illuminating time in the devices using *s*MoO$_3$ (5 nm) and PEDOT:PSS (40 nm) based solar cells.
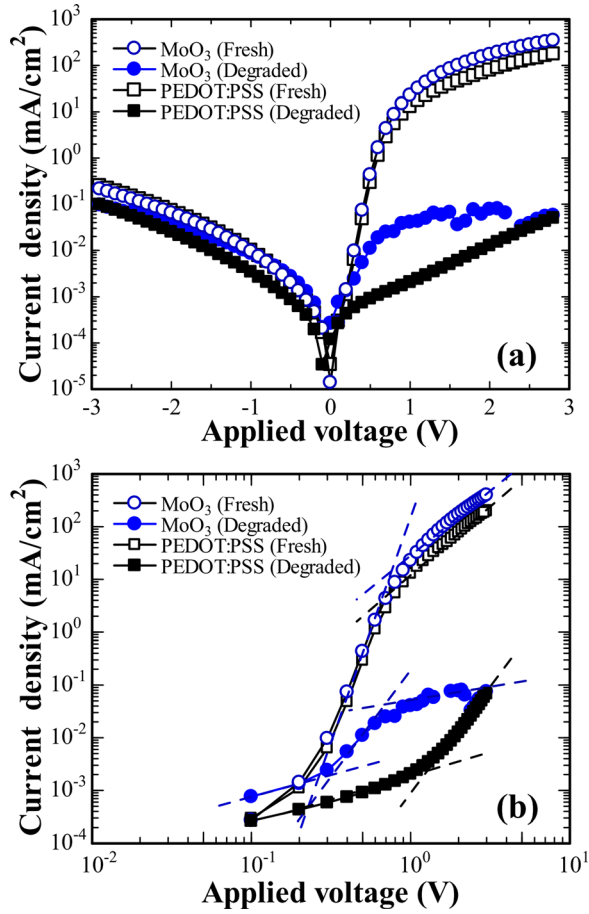
FIG. 3. *J-V* characteristics of *s*MoO$_3$ (5 nm) and PEDOT:PSS (40 nm) based solar cells (fresh and 1 h degraded devices) for (a) linear plot and (b) double logarithmic plot.

subsequently (>0.7 V) go through a transition region towards a V^2 dependence that can be described by Mott' model of space charge limited current (SCLC). For degraded devices, the reverse currents nearly did not change. However, serious deterioration for forward currents was observed in both devices, especially in PEDOT:PSS-based device. The overall currents decreased by three orders of magnitude compared to those in fresh devices. The slopes of the *J-V* curves are about 4 in this region. Particularly, transition region towards V^2 dependence for the current did not appear in PEDOT:PSS-based device. The deterioration of *J-V* curves in degraded devices is assumed to be associated with the energy-dependent traps distribution due to the active layer degradation and the interface change due to the unstable interfacial layer.

Furthermore, energy-dependent traps distribution was evaluated using a differential method. The trap density N_T is expressed as[33–37]

$$N_T = \frac{\varepsilon_i \varepsilon_0 \kappa_1 \kappa_2}{2d^2 kT} \frac{V}{n-1}, \quad (1)$$

where κ_1 is the correction factor of electric field deviation that is related to the average distance of the injected charge from the electrode ($1 \leqq \kappa_1 \leqq 2$), κ_2 is the correction factor of carrier density which relates to the ratio of the carrier concentration at the electrode to the injection carrier

concentration ($1/2 \leqq \kappa_2 \leqq 2$), the $\kappa_1 \kappa_2$ product is assumed to be unity, d the film thickness of the active layer, ε_0 the vacuum dielectric constant, and the relative dielectric constant ε_i is assumed as 3, n obeys the following relation:

$$n = \partial(\ln J)/\partial(\ln V). \quad (2)$$

The energy difference between the Fermi level E_F and the highest occupied molecular orbital (HOMO) energy level E_{HOMO} of active layer can be written as

$$-(E_{HOMO} - E_F) = \frac{kT}{q}\ln\left(\frac{d}{\kappa_1 N_0 q\mu}\right) + \frac{kT}{q}\ln\left(\frac{J}{V}\right), \quad (3)$$

where q the unit charge, k the Boltzmann constant, N_0 the effective density state at the HOMO level, and μ the hole mobility of the active layer.

Figs. 4(a) and 4(b) shows the energy-dependent bulk traps distribution in *s*MoO$_3$- and PEDOT:PSS-based cells for the condition of fresh devices and degraded devices, respectively. Two Gaussian peaks were observed in degraded devices. The Gaussian distribution at higher energies can be regarded as the contribution to the DOS in the active layer since the distribution is common to all the devices. Compared to fresh devices, additional Gaussian distributions at lower energies appeared in both degraded devices. We assumed that the additional Gaussian peak at lower energies was related to the effect of degraded hole interfacial layer on the bulk trap density. As mentioned above, interfacial conditions affected by the device fabricating circumstance such as the residual solvent strongly affect the device degradation
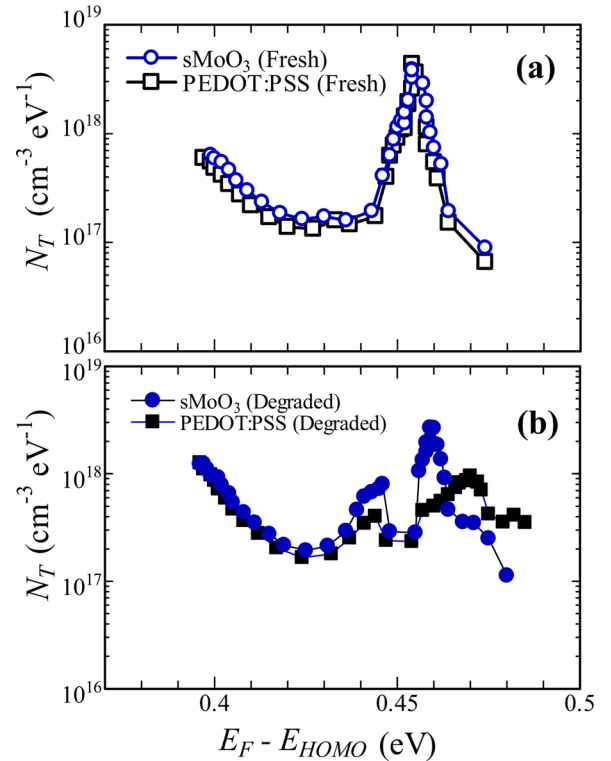

FIG. 4. Trap density distributions evaluated by a differential method in *s*MoO$_3$ (5 nm) and PEDOT:PSS (40 nm) based solar cells for (a) the fresh devices and (b) the degraded devices.

process. Additional Gaussian peak means that additional trap states were generated at the interface between the hole interfacial layer (sMoO$_3$ and/or PEDOT:PSS) and active layer. Interestingly, in the case of PEDOT:PSS-based degraded cell, the trap density distribution demonstrated a broader form and the distribution related to the active layer shifted to higher energies compared to sMoO$_3$-based degraded cell. Besides on the ITO electrode, the acidic corrosion from PEDOT:PSS also has the negative effect on the active layer, which may change the film morphology and destroys the interface contact between the PEDOT:PSS and the active layer. We assumed that the broader trap density distribution in PEDOT:PSS-based degraded cell was related to an unstable PEDOT:PSS interfacial layer compared to sMoO$_3$. Noticeably, electrode and/or other factors may have the effect on the device degradation, which can result in additional Gaussian peak appeared in degraded devices. For clarify the detailed contribution, further experiments and/or new evaluating techniques are necessary in the future.

In summary, we have investigated the influence of two different hole interfacial layer PEDOT:PSS and aqueous solution-processed MoO$_3$ on cell stability in P3HT:IC$_{60}$BA based bulk heterojunction solar cells. sMoO$_3$-based device demonstrated obviously improved stability compared to PEDOT:PSS-based one. Trap states distribution demonstrated that additional trap states were generated at the interface between the hole interfacial layer (sMoO$_3$ and/or PEDOT:PSS) and the active layer with comparing the trap states distributions in PEDOT:PSS- and sMoO$_3$-based degraded devices.

[1]M. A. Green, K. Emery, Y. Hishikawa, W. Warta, and E. D. Dunlop, Prog. Photovoltaics **20**, 12 (2012).

[2]M. Jørgensen, K. Norrman, S. A. Gevorgyan, T. Tromholt, B. Andreasen, and F. C. Krebs, Adv. Mater. **24**, 580 (2012).

[3]P. Kumar and S. Chand, Prog. Photovoltaics **20**, 377 (2012).

[4]M. O. Reese, A. Nardes, M. B. L. Rupert, R. E. Larsen, D. C. Olson, M. T. Lloyd, S. E. Shaheen, D. S. Ginley, G. Rumbles, and N. Kopidakis, Adv. Funct. Mater. **20**, 3476 (2010).

[5]J. Abad, A. Urbina, and J. Colchero, Org. Electron. **12**, 1389 (2011).

[6]F. C. Krebs, T. Tromholt, and M. Jørgensen, Nanoscale **2**, 878 (2010).

[7]S. Schäfer, A. Petersen, T. A. Wagner, R. Kniprath, D. Lingenfelser, A. Zen, T. Kirchartz, B. Zimmermann, U. Würfel, X. Feng, and T. Mayer, Phys. Rev. B **83**, 165311 (2011).

[8]G. Yu, J. Gao, J. C. Hummelen, F. Wudl, and A. J. Heeger, Science **270**, 1789 (1995).

[9]M. Wang, Q. Tang, J. An, F. Xie, J. Chen, S. Zheng, K. Y. Wong, Q. Miao, and J. Xu, ACS Appl. Mater. Interfaces **2**, 2699 (2010).

[10]A. W. Hains, J. Liu, A. B. F. Martinson, M. D. Irwin, and T. J. Marks, Adv. Funct. Mater. **20**, 595 (2010).

[11]M. F. Xu, L. S. Cui, X. Z. Zhu, C. H. Gao, X. B. Shi, Z. M. Jin, Z. K. Wang, and L. S. Liao, Org. Electron. **14**, 657 (2013).

[12]K. Norrman, S. A. Gevorgyan, and F. C. Krebs, ACS Appl. Mater. Interfaces **1**, 102 (2009).

[13]M. Lira-Cantu, K. Norrman, J. W. Andreasen, and F. C. Krebs, Chem. Mater. **18**, 5684 (2006).

[14]Z. Xu, L. M. Chen, G. W. Yang, C. H. Huang, J. H. Hou, Y. Wu, G. Li, C. S. Hsu, and Y. Yang, Adv. Funct. Mater. **19**, 1227 (2009).

[15]J. Alstrup, M. Jørgensen, A. J. Medford, and F. C. Krebs, ACS Appl. Mater. Interfaces **2**, 2819 (2010).

[16]Z. K. Wang, Y. H. Lou, H. Okada, and S. Naka, ACS Appl. Mater. Interfaces **3**, 2496 (2011).

[17]Z. K. Wang, Y. H. Lou, H. Okada, and S. Naka, AIP Adv. **1**, 032130 (2011).

[18]M. P. de Jong, L. J. van. I. Jzendoorn, and M. J. A. de Voigt, Appl. Phys. Lett. **77**, 2255 (2000).

[19]V. Shrotriya, G. Li, Y. Yao, C. W. Chu, and Y. Yang, Appl. Phys. Lett. **88**, 073508 (2006).

[20]C. Tao, S. Ruan, G. Xie, X. Kong, L. Shen, F. Meng, C. Liu, X. Zhang, W. Dong, and W. Chen, Appl. Phys. Lett. **94**, 043311 (2009).

[21]S. Murase and Y. Yang, Adv. Mater. **24**, 2459 (2012).

[22]J. J. Jasieniak, J. Seifter, J. Jo, T. Mates, and A. J. Heeger, Adv. Funct. Mater. **22**, 2594 (2012).

[23]M. F. Xu, X. B. Shi, Z. M. Jin, F. S. Zu, Y. Liu, L. Zhang, Z. K. Wang, and L. S. Liao, ACS Appl. Mater. Interfaces **5**, 10866 (2013).

[24]K. Zilberberg, S. Trost, H. Schmidt, and T. Riedl, Adv. Energy Mater. **1**, 377 (2011).

[25]J. R. Manders, S. W. Tsang, M. J. Hartel, T. H. Lai, S. Chen, C. M. Amb, J. R. Reynolds, and F. So, Adv. Funct. Mater. **23**, 2993 (2013).

[26]K. Zilberberg, H. Gharbi, A. Behrendt, S. Trost, and T. Riedl, ACS Appl. Mater. Interfaces **4**, 1164 (2012).

[27]S. Trost, K. Zilberberg, A. Behrendt, and T. Riedl, J. Mater. Chem. **22**, 16224 (2012).

[28]K. Zilberberg, J. Meyer, and T. Riedl, J. Mater. Chem. C **1**, 4796 (2013).

[29]M. F. Xu, Y. J. Liao, F. S. Zu, J. Liang, D. X. Yuan, Z. K. Wang, and L. S. Liao, J. Mater. Chem. A **2**, 9400 (2014).

[30]J. Schafferhans, A. Baumann, A. Wagenpfahl, C. Deibel, and V. Dyakonov, Org. Electron. **11**, 1693 (2010).

[31]A. Seemann, H.-J. Egelhaaf, C. J. Brabec, and J. Hauch, Org. Electron. **10**, 1424 (2009).

[32]K. Kawano and C. Adachi, Adv. Funct. Mater. **19**, 3934 (2009).

[33]S. Nešpurek and J. Sworakowski, J. Appl. Phys. **51**, 2098 (1980).

[34]Z. K. Wang, Y. H. Lou, H. Okada, and S. Naka, Appl. Phys. Lett. **98**, 063302 (2011).

[35]Y. H. Lou, Z. K. Wang, S. Naka, and H. Okada, Chem. Phys. Lett. **529**, 64 (2012).

[36]Y. H. Lou, M. F. Xu, L. Zhang, Z. K. Wang, S. Naka, H. Okada, and L. S. Liao, Org. Electron. **14**, 2698 (2013).

[37]Y. H. Lou, L. Zhang, M. F. Xu, Z. K. Wang, S. Naka, H. Okada, and L. S. Liao, Org. Electron. **15**, 299 (2014).

[38]H. Ishi, K. Sugiyama, E. Ito, and K. Seki, Adv. Mater. **11**, 605 (1999).

[39]E. Voroshazi, B. Verreet, A. Buri, R. Müller, D. D. Nuzzo, and P. Heremans, Org. Electron. **12**, 736 (2011).

[40]B. Ecker, J. C. Nolasco, J. Pallarés, L. F. Marsal, J. Posdorfer, J. Parisi, and E. Hauff, Adv. Funct. Mater. **21**, 2705 (2011).